

K-matrix and Dalitz plot analysis from FOCUS

S. Malvezzi

I.N.F.N Sezione di Milano Bicocca, Piazza della Scienza 3, 20126 Milano, Italy

Dalitz analysis is a powerful tool for physics studies within and beyond the Standard Model. In the last decade it has helped to investigate the Heavy Flavor hadronic decay dynamics and is now being applied to extract angles of the CKM Unitarity triangle. To perform such sophisticated analyses we need to model the strong interaction effects. The FOCUS experiment has performed pilot studies in the charm sector through the *K-matrix* formalism. What has been learnt from charm will be beneficial for future accurate beauty measurements. Experience and results from FOCUS are presented and discussed.

1. Introduction

Over the last years we have seen a resurrection of Dalitz plot analyses in modern Heavy Flavor experiments. This analysis tool, first applied in the charm sector, has more recently become a standard technique, used for sophisticated studies and searches for new physics in the beauty sector. Paradigmatic examples are $B \rightarrow \rho\pi$ and $B \rightarrow D^{(*)}K^{(*)}$ for the extraction of the α and γ angles of the Unitarity Triangle. Indeed, the road to go from the detected final states to the intermediate resonances can be rather insidious and complications arise in both decays. More precisely, the extraction of α in $B \rightarrow \rho\pi$ means, operatively, selecting and filtering the desired intermediate states among all the possible $(\pi\pi)\pi$ combinations, e.g. $\sigma\pi$, $f_0(980)\pi$ etc. The extraction of γ in $B \rightarrow D^{(*)}K^{(*)}$ requires, in turn, modeling the D amplitudes. This poses the problem of how to deal with strong-dynamics effects, in particular those regarding the scalar mesons. The $\pi\pi$ and $K\pi$ S-wave are characterized by broad, overlapping states: unitarity is not explicitly guaranteed by a simple sum of Breit–Wigner functions. In addition, independently of the nature of the σ , it is not a simple Breit–Wigner. The $f_0(980)$ is a Flatté-like function, and its lineshape parametrization needs a precise determination of KK and $\pi\pi$ couplings. Recent analyses of CP violation in the $B \rightarrow DK$ channel from the beauty factories have used the Cabibbo-favored mode $K_s\pi^+\pi^-$, which is common to both D^0 and \bar{D}^0 . A set of 16 two-body resonances had to be introduced to describe the $(K\pi)\pi$ and $K_s(\pi\pi)$ states in the D^0 amplitude: two *ad hoc* resonances were required to reproduce the excess of events in the $\pi\pi$ spectrum, one at the low-mass threshold, the other at 1.1 GeV^2 . Masses and widths of the two states, named σ_1 and σ_2 , were fitted to the data themselves and found to be $M_{\sigma_1} = 484 \pm 9\text{ MeV}$, $\Gamma_{\sigma_1} = 383 \pm 14$ and $M_{\sigma_2} = 1014 \pm 7\text{ MeV}$, $\Gamma_{\sigma_2} = 88 \pm 13$ in BaBar [1] and $M_{\sigma_1} = 519 \pm 6\text{ MeV}$, $\Gamma_{\sigma_1} = 454 \pm 12$ $M_{\sigma_2} = 1050 \pm 8\text{ MeV}$, $\Gamma_{\sigma_2} = 101 \pm 7$ in Belle [2]. These scalars were invoked with no reference to those found in other processes, in particular scattering data, and with no assumption as to the correctness of the physics the model embodies. This procedure of “effectively”

fitting data invites a word of caution on estimating the systematics of these measurements. A question then naturally arises: in the era of precise measurements, do we know sufficiently well how to deal with strong-dynamics effects in the analyses?

We have faced parametrization problems in the FOCUS experiment and learnt that many difficulties are already known and studied in different fields of physics, such as nuclear and intermediate-energy physics, where broad, multi-channel, overlapping resonances are treated in the *K-matrix* formalism. The effort we have had to make mainly consisted in building a bridge of knowledge and language to reach the high-energy community; our pioneering work in the charm sector might inspire future accurate studies in the beauty sector.

2. The K-matrix and P-vector formalism

A formalism for studying overlapping and many-channel resonances was proposed long ago and is based on the *K-matrix* [3, 4] parametrization. The *K-matrix* formalism provides a direct way of imposing the two-body unitarity constraint, which is not explicitly guaranteed in the simple sum of Breit–Wigners, here referred to as the *isobar model*. Minor unitarity violations are expected for narrow, isolated resonances but more severe ones exist for broad, overlapping states. This is the real advantage of the *K-matrix* approach: it heavily simplifies the formalization of any scattering problem since the unitarity of the S matrix is automatically encoded.

Originating in the context of two-body scattering, the formalism can be generalized to cover the case of production of resonances in more complex reactions [5], with the assumption that the two-body system in the final state is an isolated one and that the two particles do not simultaneously interact with the rest of the final state in the production process [4]. The validity of the assumed quasi two-body nature of the process of the *K-matrix* approach can only be verified by a direct comparison of the model predictions with data. In particular, the failure to reproduce the Dalitz

plot distribution could be an indication of the presence of relevant, neglected three-body effects.

3. The FOCUS results

3.1. The three pion analysis

The FOCUS collaboration has implemented the K -matrix approach in the D_s and $D^+ \rightarrow \pi^+\pi^-\pi^+$ analyses. It was the first application of this formalism in the charm sector. Results and details can be found in [6]. Here I only reproduce plots of the final results. In Fig. 1 and Fig. 2 the Dalitz-plot projections are shown for D_s and D^+ into three pions.

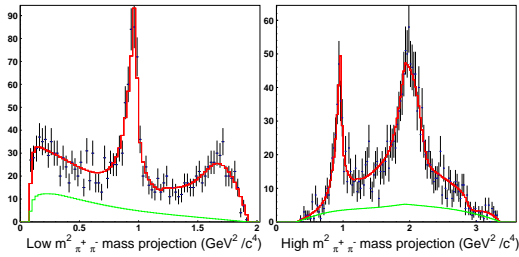


Figure 1: FOCUS D_s^+ Dalitz-plot projections with fit results superimposed. The background shape under the signal is also shown.

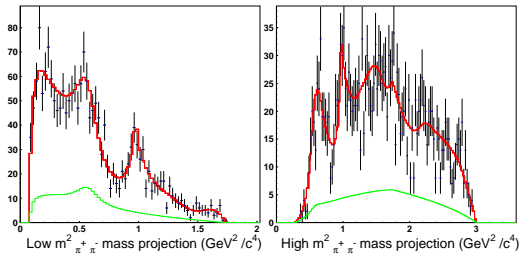


Figure 2: FOCUS D^+ Dalitz-plot projections with fit results superimposed. The background shape under the signal is also shown.

In Fig. 3 the FOCUS adaptive binning schemes for D_s^+ and D^+ are plotted. In this model [5], the production process, i.e. the D decay, can be viewed as consisting of an initial preparation of states, described by the P -vector, which then propagates according to $(I - iK\rho)^{-1}$ into the final one. The K -matrix here is the scattering matrix and is used as fixed input in our analysis. Its form was inferred by the global fit to a rich set of data performed in [7]. It is interesting to note that this formalism, beside restoring the proper dynamical features of the resonances, allows for the inclusion in D decays of the knowledge coming from scattering experiments, i.e. an enormous amount of results and science. No re-tuning of the K -matrix

parameters was needed. The confidence levels of the final fits are 3.0% and 7.7% for the D_s and D^+ respectively. The results were extremely encouraging since the same K -matrix description gave a coherent picture of both two-body scattering measurements in light-quark experiments *as well as* charm-meson decay. This result was not obvious beforehand. Furthermore, the same model was able to reproduce features of the $D^+ \rightarrow \pi^+\pi^-\pi^+$ Dalitz plot that would otherwise require an *ad hoc* σ resonance. The better treatment of the S -wave contribution provided by the K -matrix model was able to reproduce the low-mass $\pi^+\pi^-$ structure of the D^+ Dalitz plot. This suggests that any σ -like object in the D decay should be consistent with the same σ -like object measured in $\pi^+\pi^-$ scattering.

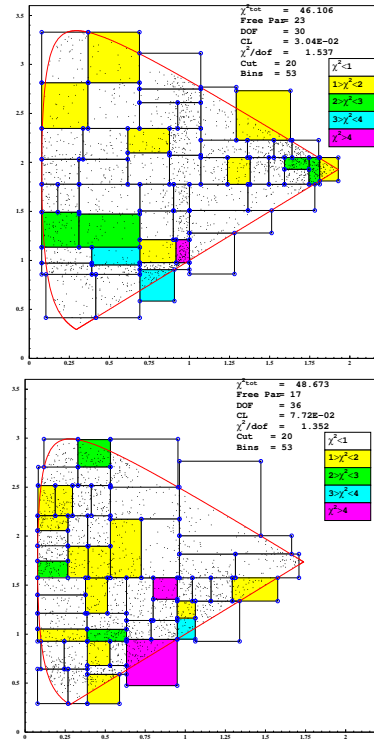


Figure 3: D_s and D^+ adaptive binning Dalitz-plots for the three pion FOCUS K -matrix fit.

Further considerations and conclusions from the FOCUS three-pion analysis were limited by the sample statistics, i.e. 1475 ± 50 and 1527 ± 51 events for D_s and D^+ respectively. We considered mandatory to test the formalism at higher statistics. This was accomplished by the $D^+ \rightarrow K^-\pi^+\pi^+$ analysis.

3.2. The $D^+ \rightarrow K^-\pi^+\pi^+$

The recent FOCUS study of the $D^+ \rightarrow K^-\pi^+\pi^+$ channel uses 53653 Dalitz-plot events with a signal fraction of $\sim 97\%$, and represents the highest statis-

tics, most complete Dalitz plot analysis for this channel. Invariant mass and Dalitz plot are shown in Fig.4.

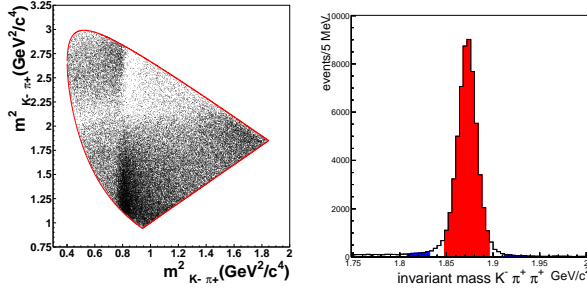


Figure 4: The $D^+ \rightarrow K^- \pi^+ \pi^+$ Dalitz plot (left) and mass distribution (right): signal and sideband regions are indicated in red and blue respectively. The sidebands are at $\pm(6-8)\sigma$ from the peak.

Details of the analysis are in [8].

An additional complication in the $K\pi$ system comes from the presence in the S -wave of the two isospin states, $I = 1/2$ and $I = 3/2$. Although only the $I = 1/2$ is dominated by resonances, both isospin components are involved in the decay of the D^+ meson into $K^- \pi^+ \pi^+$. A model for the decay amplitudes of the two isospin states can be constructed from the 2×2 K -matrix describing the $I = 1/2$ S -wave scattering in $(K\pi)_1$ and $(K\eta')_2$ (with the subscripts 1 and 2, respectively, labelling these two channels), and the single-channel K -matrix describing the $I = 3/2$ $K^- \pi^+ \rightarrow K^- \pi^+$ scattering.

The K -matrix form we use as input describes the S -wave $K^- \pi^+ \rightarrow K^- \pi^+$ scattering from the LASS experiment [9] for energy above 825 MeV and $K^- \pi^- \rightarrow K^- \pi^-$ scattering from Estabrooks *et al.* [10]. The K -matrix form follows the extrapolation down to the $K\pi$ threshold for both $I = 1/2$ and $I = 3/2$ S -wave components by the dispersive analysis by Büttiker *et al.* [11], consistent with Chiral Perturbation Theory [12]. The complete form is given below in Eqs. (4-5) with the parameters listed in Table I [13].

The total D -decay amplitude can be written as

$$\mathcal{M} = (F_{1/2})_1(s) + F_{3/2}(s) + \sum_j a_j e^{i\delta_j} B(abc|r), \quad (1)$$

where $s = M^2(K\pi)$, $(F_{1/2})_1$ and $F_{3/2}$ represent the $I = 1/2$ and $I = 3/2$ decay amplitudes in the $K\pi$ channel, j runs over vector and spin-2 tensor resonances¹, and $B(abc|r)$ are Breit-Wigner forms. The $J > 0$ resonances should, in principle, be treated in

¹Higher spin resonances have been tried in the fit with both formalisms but found to be statistically insignificant.

the same K -matrix formalism. However, the contribution from the vector wave comes mainly from the $K^*(892)$ state, which is well separated from the higher mass $K^*(1410)$ and $K^*(1680)$, and the contribution from the spin-2 wave comes from $K_2^*(1430)$ alone. Their contributions are limited to small percentages, and, as a first approximation, they can be reasonably described by a simple sum of Breit-Wigners. More precise results would require a better treatment of the overlapping $K^*(1410)$ and $K^*(1680)$ resonances as well. In accord with SU(3) expectations, the coupling of the $K\pi$ system to $K\eta'$ is supposed to be suppressed. Indeed we find little evidence that it is required. Thus $F_{1/2}$ is actually a vector consisting of two components: the first accounting for the description of the $K\pi$ channel, the second of the $K\eta'$ channel: in fitting $D^+ \rightarrow K^- \pi^+ \pi^+$ we need, of course, the $(F_{1/2})_1$ element. Its form is

$$(F_{1/2})_1 = (I - iK_{1/2}\rho)_{1j}^{-1} (P_{1/2})_j, \quad (2)$$

where I is the identity matrix, $K_{1/2}$ is the K -matrix for the $I = 1/2$ S -wave scattering in $K\pi$ and $K\eta'$, ρ is the corresponding phase-space matrix for the two channels [4] and $(P_{1/2})_j$ is the production vector in the channel j .

The form for $F_{3/2}$ is

$$F_{3/2} = (I - iK_{3/2}\rho)^{-1} P_{3/2}, \quad (3)$$

where $K_{3/2}$ is the single-channel scalar function describing the $I = 3/2$ $K^- \pi^+ \rightarrow K^- \pi^+$ scattering, and $P_{3/2}$ is the production function into $K\pi$.

Fitting of the real and imaginary parts of the $K^- \pi^+ \rightarrow K^- \pi^+$ LASS amplitude, shown in Fig. 5, and using the predictions of Chiral Perturbation Theory to continue this to threshold, gives the K -matrix parameters in Table I.

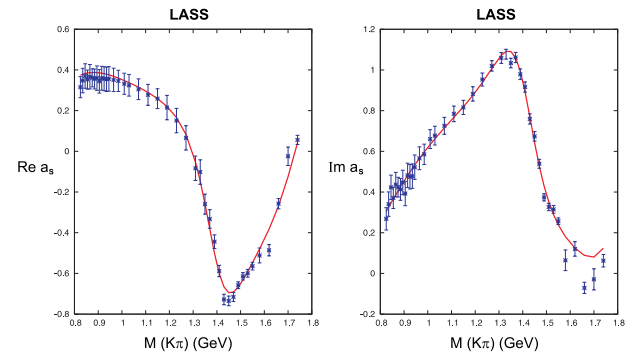


Figure 5: Real and imaginary $K^- \pi^+ \rightarrow K^- \pi^+$ amplitudes from the LASS experiment and their K -matrix fit results.

The $I = 1/2$ K -matrix is a single-pole, two-channel matrix whose elements are given in Eq. (4).

$$\begin{aligned}
K_{11} &= \left(\frac{s - s_{0\frac{1}{2}}}{s_{\text{norm}}} \right) \left(\frac{g_1 \cdot g_1}{s_1 - s} + C_{110} + C_{111}\tilde{s} + C_{112}\tilde{s}^2 \right) \\
K_{22} &= \left(\frac{s - s_{0\frac{1}{2}}}{s_{\text{norm}}} \right) \left(\frac{g_2 \cdot g_2}{s_1 - s} + C_{220} + C_{221}\tilde{s} + C_{222}\tilde{s}^2 \right) \\
K_{12} &= \left(\frac{s - s_{0\frac{1}{2}}}{s_{\text{norm}}} \right) \left(\frac{g_1 \cdot g_2}{s_1 - s} + C_{120} + C_{121}\tilde{s} + C_{122}\tilde{s}^2 \right),
\end{aligned} \tag{4}$$

where the factor of $s_{\text{norm}} = m_K^2 + m_\pi^2$ is conveniently introduced to make the individual terms in the above expression dimensionless. g_1 and g_2 are the real couplings of the s_1 pole to the first and the second channel respectively. $s_{0\frac{1}{2}} = 0.23 \text{ GeV}^2$ is the position of the Adler zero in the $I = 1/2$ ChPT elastic scattering amplitude². C_{11i} , C_{22i} and C_{12i} for $i = 0, 1, 2$ are the three coefficients of a second order polynomial for the diagonal and off-diagonal elements of the symmetric K -matrix. Polynomials are expanded around $\tilde{s} = s/s_{\text{norm}} - 1$. This form generates an S -matrix pole, which is conventionally quoted in the complex energy plane as $E = M - i\Gamma/2 = 1.408 - i0.110 \text{ GeV}$. Any more distant pole than $K_0^*(1430)$ is not reliably determined as this simple K -matrix expression does not have the required analyticity properties. Nevertheless, it is an accurate description for real values of the energy, where scattering takes place. Numerical values of the terms in Eq. (4) are reported in Table I.

The $I = 3/2$ K -matrix is given in Eq. (5). Its form is derived from a simultaneous fit to LASS data [9] and to $K^-\pi^- \rightarrow K^-\pi^-$ scattering data [10]. It is a non-resonant, single-channel scalar function.

$$K_{3/2} = \left(\frac{s - s_{0\frac{3}{2}}}{s_{\text{norm}}} \right) (D_{110} + D_{111}\tilde{s} + D_{112}\tilde{s}^2). \tag{5}$$

In Eq. (5) $s_{0\frac{3}{2}} = 0.27 \text{ GeV}^2$ is the Adler zero position in the $I = 3/2$ ChPT elastic scattering and the values of the polynomial coefficients are $D_{110} = -0.22147$, $D_{111} = 0.026637$, and $D_{112} = -0.00092057$ [13].

When moving from scattering processes to D -decays, the production P -vector has to be introduced. While the K -matrix is real, P -vectors are in general complex reflecting the fact that the initial coupling $D^+ \rightarrow (K^-\pi^+)\pi_{\text{spectator}}^+$ need not be real. The P -vector has to have the same poles as the K -matrix, so that these cancel in the physical decay amplitude. Their functional forms are:

$$(P_{1/2})_1 = \frac{\beta g_1 e^{i\theta}}{s_1 - s} + (c_{10} + c_{11}\hat{s} + c_{12}\hat{s}^2)e^{i\gamma_1} \tag{6}$$

$$(P_{1/2})_2 = \frac{\beta g_2 e^{i\theta}}{s_1 - s} + (c_{20} + c_{21}\hat{s} + c_{22}\hat{s}^2)e^{i\gamma_2} \tag{7}$$

$$P_{3/2} = (c_{30} + c_{31}\hat{s} + c_{32}\hat{s}^2)e^{i\gamma_3}. \tag{8}$$

$\beta e^{i\theta}$ is the complex coupling to the pole in the ‘initial’ production process, g_1 and g_2 are the couplings as given by Table I. The $K\pi$ mass squared $s_c = 2 \text{ GeV}^2$ corresponds to the center of the Dalitz plot. It is convenient to choose this as the value of s about which the polynomials of Eqs. (6-8) are expanded, by defining $\hat{s} = s - s_c$. The polynomial terms in each channel are chosen to have a common phase γ_i to limit the number of free parameters in the fit and avoid uncontrolled interference among the physical background terms. Thus, the coefficients of the second order polynomial, c_{ij} , are real. Coefficients and phases of the P -vectors, except g_1 and g_2 , are the only free parameters of the fit determining the scalar components.

Free parameters for vectors and tensors are amplitudes and phases (a_i and δ_i). $K\pi$ scattering determines the parameters of the K -matrix elements and these are fixed inputs to this D decay analysis. Table II reports our K -matrix fit results. It shows quadratic terms in $(P_{1/2})_1$ are significant in fitting data, while in both $(P_{1/2})_2$ and $P_{3/2}$ constants are sufficient.

The $J > 0$ states required by the fit are listed in Table III.

The S -wave component accounts for the dominant portion of the decay ($83.23 \pm 1.50\%$). A significant fraction, $13.61 \pm 0.98\%$, comes, as expected, from $K^*(892)$; smaller contributions come from two vectors $K^*(1410)$ and $K^*(1680)$ and from the tensor $K_2^*(1430)$. It is conventional to quote fit fractions for each component and this is what we do. Care should be taken in interpreting some of these since strong interference can occur. This is particularly apparent between contributions in the same-spin partial wave. While the total S -wave fraction is a sensitive measure of its contribution to the Dalitz plot, the separate fit fractions for $I = 1/2$ and $I = 3/2$ must be treated with care. The broad $I = 1/2$ S -wave component inevitably interferes strongly with the slowly varying $I = 3/2$ S -wave, as seen for instance in [14]. Fit results on the projections are re shown in Fig. 6. The corresponding adaptive binning scheme is at the top of Fig. 7.

The fit $\chi^2/\text{d.o.f}$ is 1.27 corresponding to a confidence level of 1.2%. If the $I = 3/2$ component is removed from the fit, the $\chi^2/\text{d.o.f}$ worsens to 1.54, corresponding to a confidence level of 10^{-5} .

² Chiral symmetry breaking demands an Adler zero in the elastic S -wave amplitudes in the unphysical region. ChPT at next-to-leading order fixes these positions s_{0I} [11, 12].

Table I Values of parameters for the $I = 1/2$ K -matrix.

pole (GeV ²)	coupling (GeV)	C_{11i}	C_{12i}	C_{22i}
$s_1 = 1.7919$	$g_1 = 0.31072$ $g_2 = -0.02323$	$C_{110} = 0.79299$ $C_{111} = -0.15099$ $C_{112} = 0.00811$	$C_{120} = 0.15040$ $C_{121} = -0.038266$ $C_{122} = 0.0022596$	$C_{220} = 0.17054$ $C_{221} = -0.0219$ $C_{222} = 0.00085655$

 Table II S -wave parameters from the K -matrix fit to the FOCUS $D^+ \rightarrow K^- \pi^+ \pi^+$ data. The first error is statistic, the second error is systematic from the experiment, and the third is systematic induced by model input parameters for higher resonances. Coefficients are for the unnormalized S -wave.

coefficient	phase (deg)
$\beta = 3.389 \pm 0.152 \pm 0.002 \pm 0.068$	$\theta = 286 \pm 4 \pm 0.3 \pm 3.0$
$c_{10} = 1.655 \pm 0.156 \pm 0.010 \pm 0.101$	$\gamma_1 = 304 \pm 6 \pm 0.4 \pm 5.8$
$c_{11} = 0.780 \pm 0.096 \pm 0.003 \pm 0.090$	
$c_{12} = -0.954 \pm 0.058 \pm 0.0015 \pm 0.025$	
$c_{20} = 17.182 \pm 1.036 \pm 0.023 \pm 0.362$	$\gamma_2 = 126 \pm 3 \pm 0.1 \pm 1.2$
$c_{30} = 0.734 \pm 0.080 \pm 0.005 \pm 0.030$	$\gamma_3 = 211 \pm 10 \pm 0.7 \pm 7.8$
<i>Total S-wave fit fraction</i> = $83.23 \pm 1.50 \pm 0.04 \pm 0.07$ %	
<i>Isospin 1/2 fraction</i> = $207.25 \pm 25.45 \pm 1.81 \pm 12.23$ %	
<i>Isospin 3/2 fraction</i> = $40.50 \pm 9.63 \pm 0.55 \pm 3.15$ %	

 Table III Fit fractions, phases, and coefficients for the $J > 0$ components from the K -matrix fit to the FOCUS $D^+ \rightarrow K^- \pi^+ \pi^+$ data. The first error is statistic, the second error is systematic from the experiment, and the third error is systematic induced by model input parameters for higher resonances.

component	fit fraction (%)	phase δ_j (deg)	coefficient
$K^*(892)\pi^+$	13.61 ± 0.98 $\pm 0.01 \pm 0.30$	0 (fixed)	1 (fixed)
$K^*(1680)\pi^+$	1.90 ± 0.63 $\pm 0.009 \pm 0.43$	1 ± 7 $\pm 0.1 \pm 6$	0.373 ± 0.067 $\pm 0.009 \pm 0.047$
$K_2^*(1430)\pi^+$	0.39 ± 0.09 $\pm 0.004 \pm 0.05$	296 ± 7 $\pm 0.3 \pm 1$	0.169 ± 0.017 $\pm 0.010 \pm 0.012$
$K^*(1410)\pi^+$	0.48 ± 0.21 $\pm 0.012 \pm 0.17$	293 ± 17 $\pm 0.4 \pm 7$	0.188 ± 0.041 $\pm 0.002 \pm 0.030$

These results can be compared with those obtained in the effective isobar model, which can serve as the standard for fit quality. Projections are shown in Fig. 8 and the adaptive binning scheme at the bottom of Fig. 7.

Two *ad hoc* scalar resonances are required, of mass 856 ± 17 and 1461 ± 4 and width 464 ± 28 and 177 ± 8 MeV/ c^2 respectively. A detailed discussion of the results and the systematics can be found in [8]. The results of the K -matrix fit showed that a consistent representation with scattering is possible, the global fit quality being indeed good. However, it deteriorates

at higher $K\pi$ mass. This is not surprising since our K -matrix treatment only includes two channels $K\pi$ and $K\eta'$. While we have reliable information on the former channel, we have relatively poor constraints on the latter. This means that as we consider $K\pi$ masses far above $K\eta'$ threshold, these inadequacies in the description of the $K\eta'$ channel become increasingly important. This is expected to become worse as yet further inelastic channels open up. Consequently, improvements could be made by using a number of D -decay chains with $K\pi$ final state interactions and inputting all these in one combined analysis in which

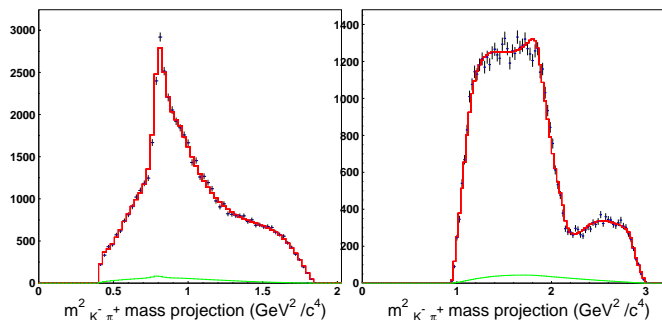


Figure 6: The Dalitz plot projections with the K -matrix fit superimposed. The background shape under the signal is also shown.

several inelastic channels are included in the K -matrix formalism. In the present single $D^+ \rightarrow K^- \pi^+ \pi^+$ channel, adding further inelastic modes would be just adding free unconstrained parameters for which there is little justification. It is interesting to note that the adaptive binning scheme shows that both the K -matrix and the isobar fit are not able to reproduce data well in the region at 2 GeV², in the vicinity of the $K\eta'$ threshold. It is also the energy domain where higher spin states live. Vector and tensor fit parameters in the two models are in very good agreement: we do not exclude the possibility that a better treatment of these amplitudes could improve the χ^2 . Some isolated spots of high χ^2 could be caused by an imperfect modeling of the efficiency as they are in the same regions in both fits.

A feature of the K -matrix amplitude analysis is that it allows an indirect phase measurement of the separate isospin $I = 1/2$ which should be compared with the same $I = 1/2$ LASS phase, extrapolated from 825 GeV down to threshold according to Chiral Perturbation Theory. This is done in the right plot of Fig. 9. In this model [5] the P -vector allows for a phase variation accounting for the interaction with the third particle in the process of resonance formation. It so happens that the Dalitz fit gives a nearly constant production phase. The two phases in Fig. 9b) have the same behaviour up to ~ 1.1 GeV. However, approaching $K\eta'$ threshold, effects of inelasticity and differing final state interactions start to appear.

The difference between the phases in Fig. 9a) is due to the $I = 3/2$ component.

These results are consistent with $K\pi$ scattering data, and consequently with Watson's theorem predictions for two-body $K\pi$ interactions in the low $K\pi$ mass region, up to ~ 1.1 GeV, where elastic processes dominate. This means that possible three-body interaction effects, not accounted for in the K -matrix parametrization, play a marginal role.

Our results for the total S -wave are in general agreement with those from the E791 analysis, in which the

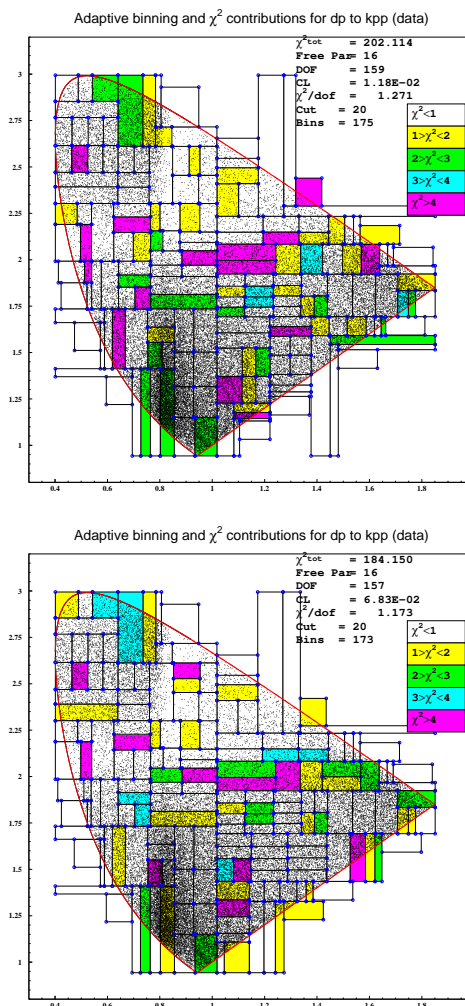


Figure 7: The adaptive binning schemes corresponding to the K -matrix (top) and isobar (bottom) fits.

S -wave modulus and phase were determined in each $K\pi$ slice [15], [16]. What does this analysis contribute to the discussion of the existence and parameters of the κ ? We know from analysis [17] of the LASS data (which in $K^- \pi^+$ scattering only start at 825 MeV) there is no pole, the $\kappa(900)$, in its energy range. However, below 800 MeV, deep in the complex plane, there is very likely such a state. Its precise location requires a more sophisticated analytic continuation onto the unphysical sheet than the K -matrix representation provided here. This is because of the need to approach close to the crossed channel cut, which is not correctly represented for a robust analytic continuation. However, our K -matrix representation fits along the real energy axis inputs on scattering data and Chiral Perturbation Theory in close agreement with those used in the analysis by Descotes-Genon and Moussallam [18] that locates the κ with a mass of (658 ± 13) MeV and a width of (557 ± 24) MeV by careful continuation. These pole parameters are quite different from those

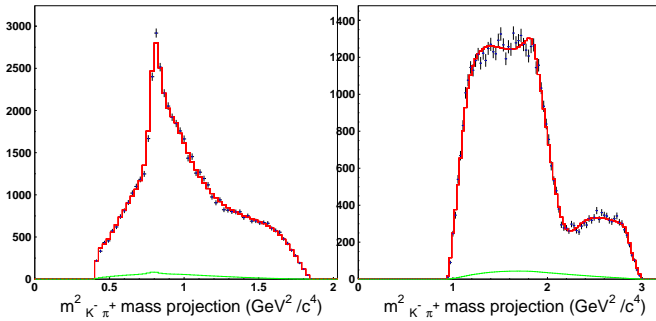


Figure 8: Dalitz plot projections with our isobar fit superimposed. The background shape under the signal is also shown.

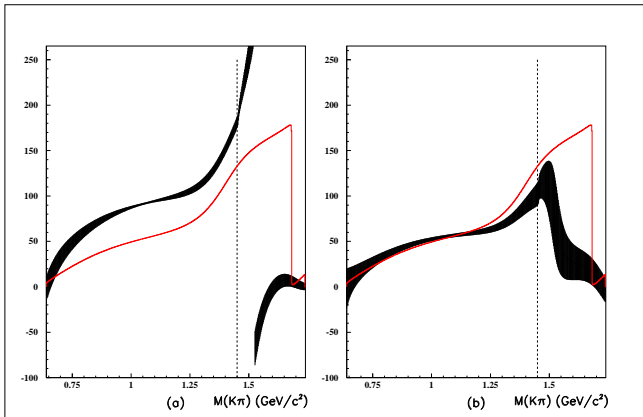


Figure 9: Comparison between the LASS $I = 1/2$ phase + ChPT (continuous line) and the F -vector phases (with $\pm 1\sigma$ statistical error bars); a) total F -vector phase; b) $I = 1/2$ F -vector phase. The vertical dashed line shows the location of the $K\eta'$.

implied by the simple isobar fits. We have thus shown that whatever κ is revealed by our $D^+ \rightarrow K^-\pi^+\pi^+$ results, it is the same as that found in scattering data. Consequently, our analysis supports the conclusions of [18] and [19].

4. Conclusions

Dalitz-plot analysis represents a unique, powerful and promising tool for studying the Heavy Flavor decay dynamics. There is a recent, vigorous effort to perform amplitude analysis: a more robust formalism has been implemented, many channels have been investigated. The beauty community can benefit from charm experience and expertise. The high statistic $D^+ \rightarrow K^-\pi^+\pi^+$ from FOCUS showed us that D -decay can also teach us about $K\pi$ interaction much

closer to threshold than the older scattering results. This serves as a valuable check from experiment [20] of the inputs to the analyses of [18] and [19] based largely on theoretical considerations. Dalitz-plot analysis will definitely keep us company over the next few years. There will be a lot of work for both experimentalists and theorists alike: synergy will be invaluable. Some complications have already emerged, especially in the charm field, others, unexpected, will only become clearer when we delve deeper into the beauty sector. B_s will be a completely new chapter. The analysis is challenging but there are no shortcuts toward ambitious and high-precision studies and, ultimately, to New Physics searches.

References

- [1] B. Aubert *et al.*, Phys. Rev. Lett. **95** (2005) 121802.
- [2] A. Poluektov *et al.*, Phys. Rev. **D73** (2006) 112009.
- [3] E. P. Wigner, Phys. Rev. **70** (1946) 15.
- [4] S. U. Chung *et al.*, Annalen Phys. **4** (1995) 404.
- [5] I. J. R. Aitchison, Nucl. Phys. **A189**, (1972) 417.
- [6] J. M. Link *et al.*, Phys. Lett. **B585** (2004) 200.
- [7] V. V. Anisovich and A. V. Sarantsev, Eur. Phys. J. A **16**, 229 (2003).
- [8] J. M. Link *et al.*, Phys. Lett. **B653** (2007) 1.
- [9] D. Aston *et al.*, Nucl. Phys. **B296** (1988) 493.
- [10] P. Estabrooks *et al.*, Nucl. Phys. **B133** (1978) 490.
- [11] P. Büttiker, S. Descotes-Genon and B. Moussallam, Nucl. Phys. Proc. Suppl. **133** (2004) 223; Eur. Phys. J. **C33** (2004) 409.
- [12] V. Bernard, N. Kaiser and U. G. Meißner, Phys. Rev. **D43** (1991) 2757; Nucl. Phys. **B357** (1991) 129.
- [13] M. R. Pennington, private communication.
- [14] L. Edera, M. R. Pennington, Phys. Lett. **B623** (2005) 55.
- [15] E. M. Aitala *et al.*, Phys. Rev. **D73** (2006) 032004.
- [16] M. R. Pennington, Int. J. Mod. Phys. **A21** (2006) 5503.
- [17] S. N. Cherry and M. R. Pennington, Nucl. Phys. **A688** (2001) 823.
- [18] S. Descotes-Genon and B. Moussallam, Eur. Phys. J. **C48** (2006) 553.
- [19] Z.Y. Zhou and H.Q. Zheng, Nucl. Phys. **A775** (2006) 212.
- [20] S. Malvezzi and M. R. Pennington (in preparation).

Adaptive binning and χ^2 contributions for dp to ppp (data)

